# NON-LINEAR LAND SUBSIDENCE IN MORELIA, MEXICO, IMAGED THROUGH SYNTHETIC APERTURE RADAR INTERFEROMETRY

**Francesca Cigna [1,*], Batuhan Osmanoğlu [1,†], Enrique Cabral-Cano [2], Timothy H. Dixon [1,‡], Shimon Wdowinski [1]**

*[1] Division of Marine Geology and Geophysics, University of Miami, 4600 Rickenbacker Causeway, Miami, FL 33149-1098, USA, Email: francesca.cigna@gmail.com*
*[2] Departamento de Geomagnetismo y Exploración, Instituto de Geofísica, Universidad Nacional Autónoma de México. Ciudad Universitaria, 04510 México D.F., México*

*[*] Present address: Department of Earth Sciences, University of Firenze, Via La Pira 4, 50121 Firenze, Italy*
*[†] Present address: Geophysical Institute, University of Alaska, 903 Koyukuk Dr., Fairbanks, Alaska 99775-7320, USA*
*[‡] Present address: Department of Geology, University of South Florida, 4202 E. Fowler Avenue, SCA 528, Tampa, FL 33620-8100, USA*

## ABSTRACT

Land subsidence affecting the city of Morelia in 2003-2010 is imaged with 23 ENVISAT scenes. Newly developed subsidence is recognized in the Rio Grande meander area, where thick compressible deposits suffer from accelerated aquifer compaction induced by recent groundwater extractions. Persistent Scatterer (PS) analyses using linear and quadratic deformation models both result in low density of targets, while small-baseline interferograms show good coherence over the whole area. At the location of Prados Verdes II well, located in the center of this subsidence feature, -10 to -15 mm/yr LOS velocities are measured in 2003-2004, accelerating to -30 mm/yr in 2004-2005, -40 to -50 mm/yr in 2006-2007, and -60 to -70 mm/yr in 2008-2009. Along the vertical direction, cumulative deformation in 2003-2009 at the water well location is estimated at -280 mm. Accelerations as high as -1 to -1.5 mm/yr$^2$ are observed by PS for the time period 2003-2010.

## 1. INTRODUCTION

Subsidence and faulting has affected several cities in central Mexico for decades, causing severe damages to their urban infrastructure and housing structures [1-3]. The city of Morelia, capital of the state of Michoacán, derives most of its water resources from local aquifers and since the early 1980s is experiencing land subsidence associated with groundwater over-exploitation, leading to declining groundwater levels, compaction and loss of porosity in the aquifer, and ultimately land subsidence and surface faulting. Past tectonics related to the Morelia-Acambay fault system controlled the overall development of the region and the formation of its horst-graben structure with variable thickness of sediment and volcanic products infill. Local stratigraphic and structural conditions also play an important role in the development and extension of subsidence-induced shallow faulting [4-6].

Synthetic Aperture Radar Interferometry (InSAR) and Persistent Scatterer Interferometry (PSI) were used to investigate spatial and temporal patterns of land subsidence affecting Morelia in 2003-2010. Reference [5] presents the results of these analyses for the whole city and compares PSI and InSAR observations with GPS, geological and groundwater extraction data.
This work focuses on a newly developed subsidence feature in the area of Rio Grande river (Fig. 1), and employs both linear and quadratic deformation models during the PSI processing. Outcomes from the time-lapse conventional InSAR are also exploited to observe temporal variations of the analyzed area and reveal accelerated motion since 2005. The observed deformation patterns for the Rio Grande meander area represent a potential source of further fault-induced structural damages for housing and urban infrastructure in the next years.

## 2. RIO GRANDE MEANDER AREA

Crossing the urban area in the NE-SW direction, the Rio Grande river flows on Quaternary sedimentary deposits and cemented tuffs of variable thickness (from few tens up to 150-200 m), on which most of the Morelia urban area has been built since the 16$^{th}$ century. Within the city, the river's course develops on the hanging wall of one of the major NE-SW trending normal faults recognized within the urbanized area, the Central Camionera fault. The presence of this fault configures a stepped morphology, with a sharp change of the compressible deposits thicknesses from the footwall (~30-40 m) to the hanging wall (~150 m) of the fault.
Both the presence of significant total thickness of fine-grained deposits in the saturated portion of the aquifer and the static level declines are needed to manifest compaction; aquifer compaction depends not only on the compressibility of fine-grained deposits, but also on water level changes. 40% of the city's potable water supply is extracted from 108 water wells distributed throughout the entire urban area, more than half of

*Proc. 'Fringe 2011 Workshop', Frascati, Italy,*
*19–23 September 2011 (ESA SP-697, January 2012)*

which were built or reactivated in the last 15 years. Three of them are identified within the area of the Rio Grande meander (Fig. 1): Prados Verdes II, Mariano Escobedo I and Mariano Escobedo II.

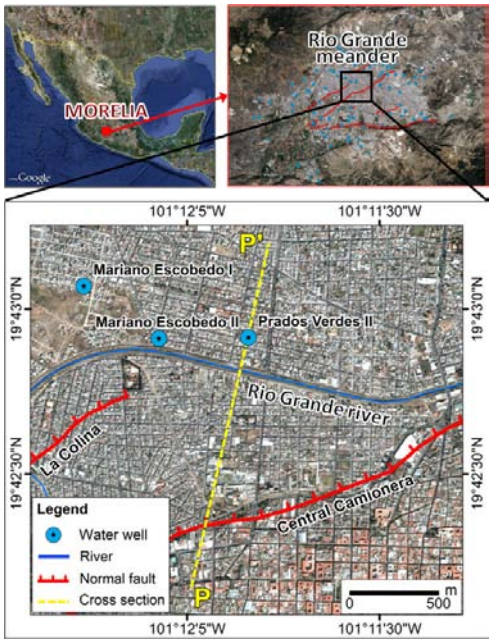


*Figure 1. Location of the Rio Grande meander area, Morelia, Mexico. Water wells and cross section P-P' are also shown.*

According to groundwater extraction data distributed by the water management agency of Morelia, OOAPAS (*Organismo Operador de Agua Potable, Alcantarillado y Saneamiento*), Prados Verdes II well was rehabilitated in 2001 as a 24 hour/day service, and with measured static water level and extraction rate of 21 m and 8 l/s, respectively. In 2005, following the installation of a new 8" casing (the previous one had a 10" diameter), the length of the pipe increased from 96 to 102 m, and the static level decreased to 22.5 m (i.e., depth to water below land surface). An increase of the water extraction rates likely occurred after the recasing, as well as further depletion of the static level; unfortunately, no further measurements are available since 2005 [5]. Applying linear interpolation on the available static level measurements since 1999, a decrease of 0.35 m/yr is observed for this well; static level is assumed to be ~24.5 m in 2011.

For Mariano Escobedo I well, constructed in 1989, less extraction data and information are available; measured extraction rates in 1989 and 1992 were 8 and 9 l/s respectively, while static level decreased from 28.4 m in 1989 to 30 m in 1992 (decline rate of 0.53 m/yr).

Rehabilitated in 1997, Mariano Escobedo II well shows decrease of the static level from 42 m in 2001, to 45 m in 2003, corresponding to a decline of 1.5 m/yr; no extraction rate measurements are available.

### 2.1. SAR data and interferometric analysis

Twenty three ENVISAT ASAR (Advanced SAR) images acquired in C-band with wavelength $\lambda$=5.6 cm (frequency $f$=5.3 GHz) are analyzed over the study area (Fig. 2). These scenes were acquired in Image Mode S2 (look angle, $\theta$=20.8°; swath=100 km) descending mode, with VV polarization, and span the interval between 12/07/2003 and 01/05/2010.

GAMMA SAR software was used to focus raw data to Single Look Complex (SLC) images [7]; DORIS (Delft Object-oriented Radar Interferometric Software) and the PSI Toolbox developed by TU-Delft were employed to perform the InSAR and PSI analyses [8], using the Automated DORIS Environment (ADORE), developed by the Geodesy Laboratory at the University of Miami (http://code.google.com/p/adore-doris/).

Four differential interferograms with short perpendicular baselines ($B_{perp}$ < 200 m) and relatively short temporal baseline ($B_{temp}$ < 1.5 yr) were used to investigate time variable deformation in 2003-2009 (Fig. 2). Their master and slave images, and respective perpendicular baselines are distributed as follows:

- ***A**: 12 Jul 2003 – 13 Nov 2004, $B_{perp}$=10.3 m*
- ***B**: 18 Dec 2004 – 3 Dec 2005, $B_{perp}$=-60.0 m*
- ***C**: 11 Feb 2006 – 27 Jan 2007, $B_{perp}$=196.6 m*
- ***D**: 27 Dec 2008 – 3 Oct 2009, $B_{perp}$=-11.9 m*

Interferograms spanning the rainy season (May-August) tended to have strong atmospheric-related artifacts and were avoided.

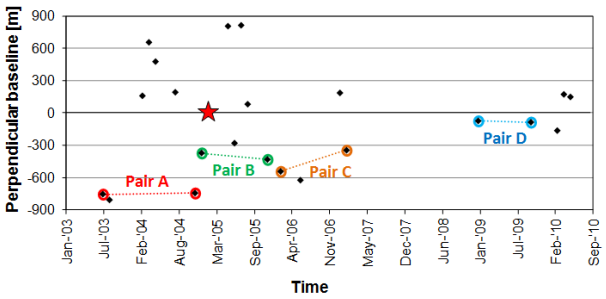


*Figure 2. Temporal and perpendicular baselines of ENVISAT ASAR IS2 descending data between 2003 and 2010, referred to the PSI master image (22 January 2005; red star). ASAR pairs A, B, C and D, selected for the time-lapse InSAR analysis are highlighted in red, green, orange and blue respectively.*

After co-registration of slave scenes to their masters, a multi-look ratio of 5:1 (final pixel size 20 m by 20 m) was used to generate raw interferograms and subsequent products. Extraction of the displacement phase component from each of the raw interferograms was carried out using the 'two-pass interferometry' approach and subtracting the topographic information with a synthetic topographic phase simulated using the 30 m

resolution ASTER Global DEM, distributed by NASA's Land Process Distributed Active Archive Center. Adaptive filtering was applied to each differential interferogram to reduce phase noise and improve subsequent 2D phase unwrapping. The Statistical-cost, Network-flow Algorithm for PHase Unwrapping (SNAPHU) approach was employed to resolve ambiguous wrapped phase data [9]. The unwrapped differential phases were converted into ground displacement maps (along the satellite Line Of Sight, LOS) and finally geocoded. Conversion to time-normalized LOS velocities was also applied, based on the time span of each interferogram.

The PSI analysis used the full multi-temporal stack of ASAR images to generate time-series of ground deformations for individual radar targets (i.e., the Persistent Scatterers, PS), subject to the condition that a model for the time history of deformation was assumed.

The scene acquired on 22/01/2005 was selected as the master, to minimize the effects of spatial and temporal decorrelation, and all the SLCs were oversampled by a factor of two in both range and azimuth (final pixel size 2 m by 10 m), to prevent undersampling of the data during co-registration to the master.

First order PS Candidates (PSC) and PS Potential (PSP) were selected using the amplitude dispersion criterion and thresholds of dispersion index of 0.3 and 0.4, respectively. Two different PSI processing were performed, using different models of phase variation through time for estimation of phase components related to deformation: first a simple linear model, and then a quadratic function, more suitable to describe accelerated motion patterns.

The reference point used for both InSAR and PSI analyses was set south of La Paloma fault (an area assumed to be devoid of large subsidence displacements) and close to the MOGA GPS station whose vertical time series exhibits stable behaviour [5].

### 2.2. Results and discussion

For the whole urban area, the deformation field observed through PSI in 2003-2010 reflects both control from past tectonics and influence from intense groundwater extraction. Subsiding areas are distributed as either concentrated circular patterns centered around water wells, or as elongate patterns parallel to faults (e.g., La Colina, La Paloma and Central Camionera). High subsidence rates are measured on the hanging wall of major normal faults coinciding with the thickest sediment deposits. Strong contrasts in subsidence rates are identified across major basin-bounding faults [5].

For more than 90% of the city, the use of a simple linear model for deformation fits the phase data extremely well; exceptions are the hanging wall of La Colina fault, and the Rio Grande meander area (Fig. 3). Despite favorable morphology and land use of this area (presence of good radar reflectors), very low PS density is observed in the buffer area 1 km large on the hanging wall side of the Central Camionera fault, especially in proximity of the Prados Verde II water well. Low LOS velocities are revealed on the footwall of the fault (up to few mm/yr), while the available PS on the hanging wall show LOS velocity up to -20 mm/yr in a concentrated area located 750 m south of the well and close to the fault trace. NW of the Prados Verde II well, measured velocities decrease as a function of distance from the well location.

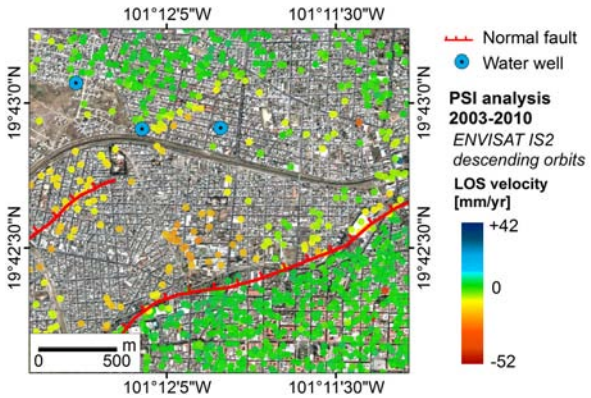


*Figure 3. LOS yearly velocity observed in 2003-2010 for the PS identified in the area of Rio Grande meander using a simple linear function to model deformation phases.*

Time-lapse analysis with InSAR reveals accelerations of subsidence in the central sector of the city, both N of the La Colina fault and in the meander area of the Rio Grande river (Fig. 4). In this latter area, well-defined patterns and very high displacements are identified, corresponding to the location of the Prados Verdes II water well [5].

The lack of PS targets using the linear model to describe deformation phase components may reflect the temporal evolution of ground displacement here, where deformation appears to be accelerating in recent years, such that the linear model applied successfully in other regions may not apply to this sector of the city. Points exhibiting strong non linear motion are therefore excluded from the PSC and PSP networks and subsequent steps of the PSI processing.

From the observation of the four interferograms and deformation maps (Fig. 5), it is evident that the recasing of this well has strongly influenced the subsidence rates of the area. Major displacements are observed beginning in 2005 (pair B). Up to -16 cm of cumulative LOS displacements are measured throughout the 2003-2009 period near the water extraction location (sum of contributions from pairs A, B, C and D). However, this is most likely an underestimation of the real ground motion, due to the 23-months temporal gap between pairs C (11/02/2006-27/01/2007) and D (27/12/2008-03/10/2009), and during which further deformation is

likely to have occurred. According to the displacements observed for the well location during the intervals C and D, about -55 mm/yr are estimated for the gap period between 27/01/2007-27/12/2008, corresponding to a displacement of ~ -10 cm along the LOS. Thus, a total cumulative LOS deformation occurred throughout 2003-2009 at the water well location is expected to be at least -26 cm. Assuming that ground displacement occurs only in the vertical direction, LOS estimates ($d_{LOS}$) can be converted to vertical displacements ($d_V$) following the relation $d_V=d_{LOS}/cos\theta$; with the available ENVISAT stack, this true vertical conversion corresponds to an increment of the LOS values by about +7% (i.e. total vertical cumulative displacement of ~ -28 cm).

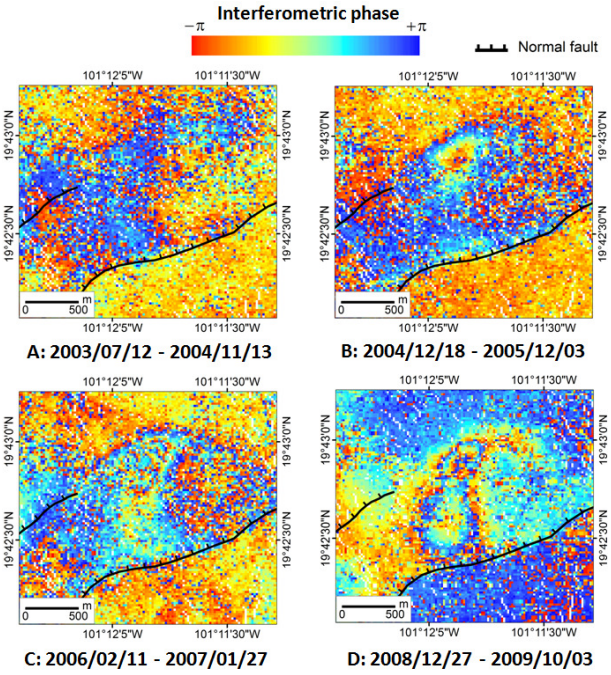


*Figure 4. Differential interferograms in the Rio Grande meander area [5]. Each fringe corresponds to 2.8 cm displacement.*

Profiles of cumulative LOS displacements, time-lapse velocities and accelerations between the different time spans are analyzed along a transect crossing both the water well and the Central Camionera fault (Fig. 6).
Deformation rates of -10 to -15 mm/yr are measured in 2003-2004. Acceleration of subsidence to -30 mm/yr is observed in 2005 at the Prados Verdes II water well location, corresponding temporally to the recasing of the well and consequent decrease of the static level. Measured rates reach -40 to -50 mm/yr in 2006-2007, and -60 to -70 mm/yr in 2008-2009. Average acceleration ranges between -10 to -15 mm/yr$^2$ in 2003-2005 and 2008-2009, while maximum values are observed in 2005-2006, reaching -25 mm/yr$^2$.

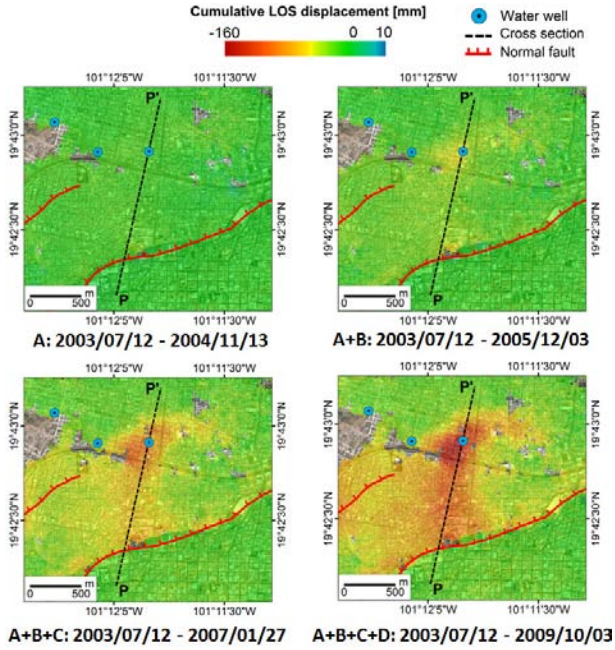


*Figure 5. Cumulative LOS deformation maps in the area of Rio Grande meander in 2003-2009.*

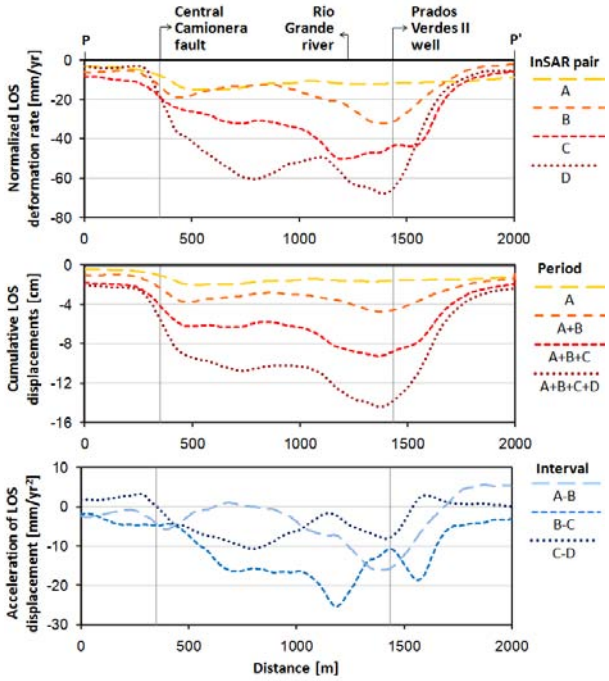


*Figure 6. Normalized LOS velocities, cumulative displacements, and acceleration observed along the profile P-P' [5].*

Two circular and adjacent areas of intense land deformation are identified in 2008-2009 (Fig. 4), suggesting the existence of either a local change of the aquifer sediment hydraulic properties which induces a decrease of subsidence between the two peak areas (hydraulically connected), or localized shallow

groundwater recharge from the Rio Grande river, which would partially counteract the local water table decrease from groundwater extraction. A sharp gradient in ground subsidence values is also observed across the Central Camionera fault, highlighting higher subsidence rates in its hanging wall block [5].

Temporal evolution of normalized deformation rates for main well and fault locations along the P-P' profile (are shown in Fig. 7. While locations P (south of Central Camionera fault), P'(NE of Prados Verdes II well) and Central Camionera fault show small variations of normalized velocities in the whole A-D period, significant acceleration is observed at the locations of both Prados Verdes II well and the Rio Grande river.

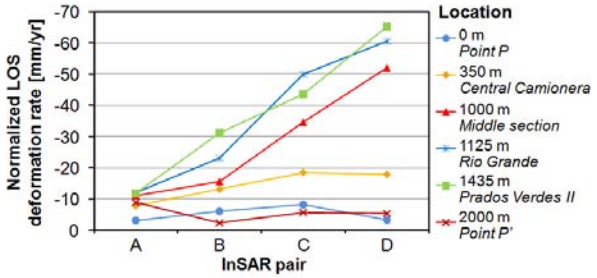


*Figure 7. Temporal evolution of normalized velocities for main locations along the P-P' profile. Locations are identified through their distance from P.*

Despite the use of a quadratic model in the improved version of the PSI processing, the density of point targets is not significantly improved in the Rio Grande meander area (Fig. 8); exceptions are the western sector of the study area (between Central Camionera and La Colina, as well as on the hanging wall of La Colina), and, partially, on the hanging wall of Central Camionera fault, south of Prados Verdes II water well. In any case the measured LOS velocities are very similar to those estimated through the application of the linear deformation model (Fig. 3).

Although measured accelerations reach -1 to -1.5 mm/yr$^2$ in the south-western sector of the meander (Fig. 9), their values differ from the estimation gathered using the InSAR analysis of one order of magnitude (InSAR pairs estimate up to -25 mm/yr$^2$ in 2005-2006). The observed discrepancy is due to both dissimilar observation time periods (2003-2010 vs. time-lapse analysis), and dissimilar locations (marginal areas vs. peak of the newly developed subsidence feature).

Persistent lack of PS in the surroundings of the water well (even after using a quadratic deformation model) is likely due to the occurrence of deformation characterized by a dissimilar behaviour from the assumed PS models (neither linear nor quadratic); a major role is also played by the occurrence of strong temporal and spatial variations of the deformation phase components, which likely compromise the phase-unwrapping process. Ambiguous nature of the 2π-wrapped phase values limits to a quarter of the wavelength (i.e. 14 mm for C-band sensors) the maximum displacement between two successive acquisitions, and two close PS of the same dataset. Thus, due to the peculiarities of the displacement patterns of in the Rio Grande meander area –rapidly variable, both spatially and temporally– some motion patterns cannot be successfully detected or they can often be underestimated by the PSI analysis [10].

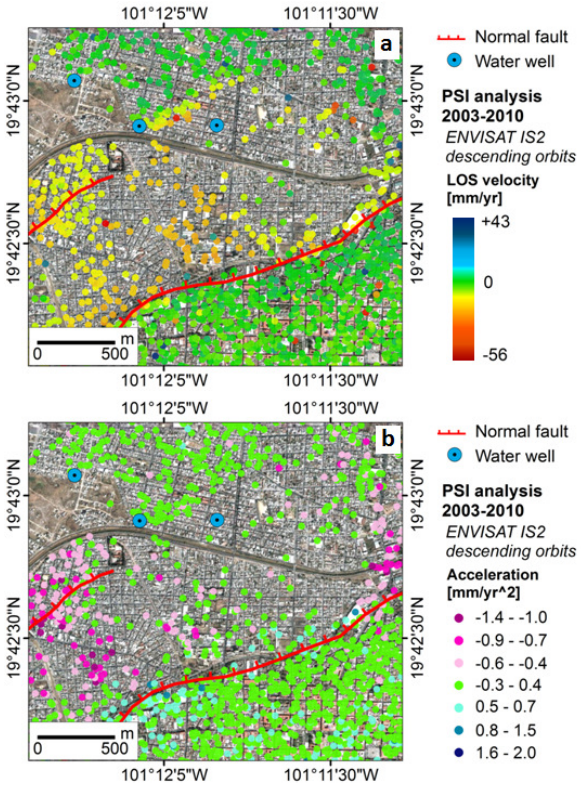


*Figure 8. LOS yearly velocity (a) and accelerations (b) observed in 2003-2010 for the PS identified in the area of Rio Grande meander using a quadratic function to model deformation phases.*

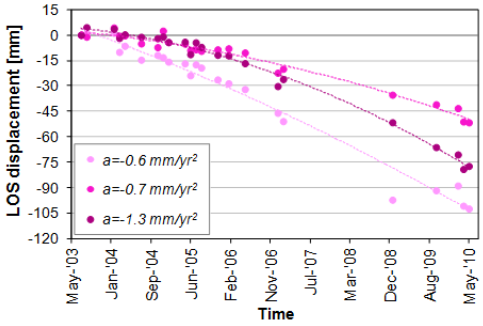


*Figure 9. Examples of PS time series obtained in the Rio Grande meander area employing a quadratic function to model ground deformation during the PSI processing. Time series are rescaled to the first acquisition (i.e. 12/07/2003).*

To improve the accuracy of the topography and deformation time series estimations, and to increase the number of measurement points within this area, the recently developed 3-D unwrapping approach using Extended Kalman Filters will be tested [11-12].
Exploitation of Small BASeline (SBAS) approach on the available ASAR stack will also be carried out to 'untie' the multi-temporal processing from the choice of an *a priori* deformation model and to better describe the evidently non-linear and accelerated motion behaviour recognized in the Rio Meander area through the time-lapse InSAR analysis.

## 3. CONCLUSIONS

InSAR and PSI analyses were used to image land subsidence in the city of Morelia in 2003-2010. A recently accelerating and well-marked subsidence feature is observed in the Rio Grande meander area, centered at the location of Prados Verdes II well.
-10 to -15 mm/yr LOS velocities are measured in 2003-2004, accelerating in 2005 (following the installation of a new casing), reaching -60 to -70 mm/yr in 2008-2009. Along the vertical direction, cumulative deformation in 2003-2009 at the water well location is estimated through InSAR as -280 mm.
Land subsidence and its induced shallow faulting will certainly become major factors to be considered when planning urban development, land use zoning and designing hazard mitigation strategies in Morelia in the next years. Despite the accelerating feature observed in the Rio Grande area, most of the city does not yet exhibit extreme subsidence rates, suggesting that improved water resource management could greatly reduce the long term subsidence.

## 4. ACKNOWLEDGEMENTS

This research is funded by UNAM (*Universidad Nacional Autónoma de México*) through PAPIIT projects IN121515, IN114907, IN117909, IN106309-2, IN108611-2 and CONACYT projects 61212 and 82868. ENVISAT ASAR data were kindly provided by ESA through CAT-1 project 1409. Many thanks go to the Delft Institute of Earth Observation and Space Systems of Delft University of Technology (TU-Delft), for making the DORIS and PSI Toolbox available.

## 5. REFERENCES

1. Cabral-Cano, E., Dixon, T.H., Miralles-Wilhelm, F., Díaz-Molina, O., Sánchez-Zamora, O. & Carande, R.E. (2008). Space geodetic imaging of rapid ground subsidence in Mexico City. *Geol. Soc. Am. Bull.* **120**(11-12), 1556-1566.

2. Osmanoğlu, B., Dixon, T.H., Wdowinski, S., Cabral-Cano, E. & Jiang, Y. (2011). Mexico City subsidence observed with persistent scatterer InSAR. *Int. J. Appl. Earth Obs. Geoinf.* **13**(1), 1-12.

3. Cigna F., Cabral-Cano E., Osmanoğlu B., Dixon T.H. & Wdowinski S. (2011). Detecting subsidence-induced faulting in Mexican urban areas by means of Persistent Scatterer Interferometry and subsidence horizontal gradient mapping. In Proc. *IGARSS 2011*, Vancouver, Canada, pp 2125-2128.

4. Garduño-Monroy, V.H., Arreygue-Rocha, E., Israde-Alcántara, I. & Rodríguez-Torres, G.M. (2001). Efectos de las fallas asociadas a sobreexplotación de acuíferos y la presencia de fallas potencialmente sísmicas en Morelia, Michoacán, México. *Revista Mexicana de Ciencias Geológicas*. **18**(1), 37-54.

5. Cigna, F., Osmanoğlu, B., Cabral-Cano, E., Dixon, T.H., Ávila-Olivera, J.A., Garduño-Monroy, V.H., DeMets, C. & Wdowinski, S. (in press). Monitoring land subsidence and its induced geological hazard with Synthetic Aperture Radar Interferometry: a case study in Morelia, Mexico. *Remote Sensing of Environment*. doi: 10.1016/j.rse.2011.09.005.

6. Cabral-Cano, E., Arciniega-Ceballos, A., Díaz-Molina, O., Cigna, F., Osmanoglu, B., Dixon, T.H., DeMets, C., Vergara-Huerta, F., Garduño-Monroy, V.H., Ávila-Olivera, J.A. & Hernández-Quintero, E. (2010). Is there a tectonic component on the subsidence process in Morelia, Mexico? In: D. Carreón-Freyre et al. (ed.), *Land subsidence, associated hazards and the role of natural resources development,* IAHS Press, pp 164-169.

7. Werner, C., Wegmüller, U., Strozzi, T. & Wiesmann, A. (2000). Gamma SAR and interferometric processing software. In Proc. *ERS-ENVISAT Symposium*, Gothenburg, Sweden, 16-20 October 2000.

8. Kampes, B. & Usai, S. (1999). Doris: The delft object-oriented radar interferometric software. In Proc. *2nd Int. Symp. Operationalization of Remote Sensing*. ITC, Enschede, The Netherlands.

9. Chen, C.W. & Zebker, H.A. (2000). Network approaches to two-dimensional phase unwrapping: intractability and two new algorithms. *J. Opt. Soc. Am. A*. **17**(3), 401-414.

10. Hanssen, R.F. (2005). Satellite radar interferometry for deformation monitoring: a priori assessment of feasibility and accuracy. *Int. J. Appl. Earth Obs. Geoinf.* **6**, 253-260.

11. Osmanoğlu, B., Dixon, T.H., Wdowinski, S. & Cabral-Cano, E. (in press). 3-D Phase Unwrapping for Satellite Radar Interferometry. In Proc. *FRINGE 2011 Workshop*, Frascati, Italy, this issue.

12. Osmanoğlu, B., Dixon, T.H., Wdowinski, S. & Biggs, J. (2009). InSAR phase unwrapping based on Extended Kalman Filtering. In Proc. *Radarcon09*, Pasadena, CA, USA. doi: 10.1109/RADAR.2009.4977028.